

# Cramér–Rao lower bounds on the performance of charge-coupled-device optical position estimators

Kim A. Winick

*Lincoln Laboratory, Massachusetts Institute of Technology, P.O. Box 73, Lexington, Massachusetts 02173*

Received September 13, 1985; accepted May 12, 1986

The problem of optically estimating an object's position by using a charge-coupled device (CCD) array composed of square pixels  $\Delta x$  on a side is analyzed. The object's image spot at the CCD is assumed to have a Gaussian intensity profile with a  $1/e$  point at a radial distance of  $\sqrt{2} \sigma_s$  from the peak, and the CCD noise is modeled as Poisson-distributed, dark-current shot noise. A two-dimensional Cramér–Rao bound is developed and used to determine a lower limit for the mean-squared error of any unbiased position estimator, and the maximum-likelihood estimator is also derived. For the one-dimensional position-estimation problem the lower bound is shown to be minimum for a pixel-to-image size ratio  $\Delta x/\sigma_s$  of between 1 and 2 over a wide range of signal-to-noise ratios. Similarly for the two-dimensional problem, the optimum ratio is shown to lie between 1.5 and 2.5. As is customary in direct detection systems, it is also observed that the lower bound is a function of both the signal power and noise power separately and not just of their ratio. Finally, the maximum-likelihood estimator is shown to be independent of the signal and noise powers at high signal-to-noise ratios.

## INTRODUCTION

There are many applications that require the precise estimation of an object's position as viewed through an optical system. Examples include star trackers for celestial navigation and spatial acquisition systems for optical links. The development of low-noise charge-coupled device (CCD) imaging arrays in the early 1970's has made it possible to perform accurate position estimates and has provided an impetus for building high-resolution tracking systems. This fact is clearly illustrated by the first Astro mission, which was to be launched in March 1986 to observe Halley's comet and several other astronomical bodies. The shuttle disaster, however, has postponed the program. The Astro payload, when launched, will include a new generation of star trackers that use CCD arrays. Star positions will be determined to accuracies of 0.2 seconds of arc over a  $2.2^\circ \times 2.5^\circ$  field of view.<sup>1</sup>

The performance of CCD position-estimation systems has been an area of recent interest, and the ability to achieve subpixel resolution has been demonstrated.<sup>1-7</sup> Most of the systems investigated to date are sophisticated peak or centroid trackers. The performance of any tracker will depend on a host of system parameters, which include signal strength, CCD noise, and image-spot size. For various suboptimum tracking algorithms, Dennison and Stanton<sup>4</sup> along with others<sup>3,7</sup> have investigated tracking performance as a function of the ratio of image-spot size to the CCD pixel size.

This paper uses classical estimation theory to determine a lower bound (i.e., a two-dimensional Cramér–Rao bound) for the mean-squared error of any unbiased position-estimation system that uses a CCD array. Furthermore, for a given CCD array, the spot-size to pixel-size ratio that yields the smallest lower bound will be derived along with the maximum-likelihood estimator.

In the analysis to follow, the CCD array will be assumed to be composed of identical square pixels without dead space, and the image spot will be represented by a Gaussian-shaped intensity profile. A Gaussian intensity distribution is assumed rather than a diffraction-limited Airy disk because it

is mathematically more tractable. Furthermore, a Gaussian profile is an excellent approximation to an Airy distribution in its central region, and if the link includes part of the atmosphere, turbulence will tend to produce a Gaussian-shaped spot in any case.

Both the one-dimensional (1-D) and two-dimensional (2-D) position-estimation problems will be analyzed below. In each case, the CCD noise will be assumed to be Poisson-distributed shot noise generated by both the image spot and the detector dark current. Background-generated shot noise will be neglected under the assumption of either nighttime operation or the use of a narrow-wavelength selective filter preceding the CCD detector. This restriction, however, can be removed easily.

The analysis presented below differs in several important respects from previously published theoretical work. This can be most clearly observed by noting that previous theoretical work generally falls into one of two categories. In the first category, Poisson-distributed shot noise is assumed to be generated only by the image spot or the image spot plus background, and the detector is assumed to have noiseless pixels (i.e., no dark current) of infinitely small size.<sup>8-11</sup> The optimum or suboptimum position estimator and its performance bounds are then derived. In the second category a fixed spot size and detector structure such as a  $2 \times 2$  quad array are assumed along with signal and dark-current shot noise. A lower bound on the performance of any unbiased estimator that uses this detector structure is then derived.<sup>12-19</sup>

Chen<sup>20</sup> and Chen and Snyder<sup>21</sup> also investigated optical position estimation but in terms of a general stochastic tracking problem. Their papers, however, do not address the issue of optimum spot size for a CCD array having fixed dark-current values and pixel widths.

## HEURISTIC ARGUMENT

Below, a simple intuitive argument is presented for why there should be a pixel-to-image spot-size ratio that minimizes the position-estimation error. First, assume that a

CCD array with a fixed pixel size and a fixed amount of dark-current shot noise per pixel is given. This is generally the case since one buys the "best" CCD array available and then must live with its characteristics. We are now free to adjust the focal length of the optical system in order to control the image-spot size at the CCD detector. To perform the most accurate estimate of position, it is best to maximize the signal energy collected and at the same time minimize the noise. Note that when the pixels are much smaller than the image-spot size this is not possible, because we must "look" at many noisy pixels in order to collect most of the signal energy in the spot. Thus the image-spot size should not be too large. On the other hand, if the spot size is very small, then it will be contained almost entirely within one pixel, and the estimator will be unable to produce subpixel resolution. Consequently, for a given CCD array there should exist some intermediate image-spot size that minimizes the position-estimation error.

**TWO-DIMENSIONAL CRAMÉR-RAO BOUND**

In this section a 2-D version of the Cramér-Rao bound (Ref. 19, pp. 79-81) will be derived. Suppose that  $\mathbf{c}$  is some observed vector quantity that is statistically related to  $\epsilon_x$  and  $\epsilon_y$ . Furthermore, let  $\hat{\epsilon}_x(\mathbf{c})$  denote an unbiased estimator of  $\epsilon_x$ . Then we can write

$$\int [\hat{\epsilon}_x(\mathbf{c}) - \epsilon_x] p(\mathbf{c}|\epsilon_x, \epsilon_y) d\mathbf{c} = 0, \tag{1}$$

$$\frac{\partial}{\partial \epsilon_x} \int [\hat{\epsilon}_x(\mathbf{c}) - \epsilon_x] p(\mathbf{c}|\epsilon_x, \epsilon_y) d\mathbf{c} = 0, \tag{2}$$

$$\int [\hat{\epsilon}_x(\mathbf{c}) - \epsilon_x] \frac{\partial p(\mathbf{c}|\epsilon_x, \epsilon_y)}{\partial \epsilon_x} d\mathbf{c} - \int p(\mathbf{c}|\epsilon_x, \epsilon_y) d\mathbf{c} = 0, \tag{3}$$

$$\int [\hat{\epsilon}_x(\mathbf{c}) - \epsilon_x] \frac{\partial \ln p(\mathbf{c}|\epsilon_x, \epsilon_y)}{\partial \epsilon_x} p(\mathbf{c}|\epsilon_x, \epsilon_y) d\mathbf{c} = \int p(\mathbf{c}|\epsilon_x, \epsilon_y) d\mathbf{c}, \tag{4}$$

$$\int [\hat{\epsilon}_x(\mathbf{c}) - \epsilon_x] \frac{\partial \ln p(\mathbf{c}|\epsilon_x, \epsilon_y)}{\partial \epsilon_x} p(\mathbf{c}|\epsilon_x, \epsilon_y) d\mathbf{c} = 1. \tag{5}$$

Similarly,

$$\frac{\partial}{\partial \epsilon_y} \int [\hat{\epsilon}_x(\mathbf{c}) - \epsilon_x] p(\mathbf{c}|\epsilon_x, \epsilon_y) d\mathbf{c} = 0, \tag{6}$$

$$\int [\hat{\epsilon}_x(\mathbf{c}) - \epsilon_x] \frac{\partial p(\mathbf{c}|\epsilon_x, \epsilon_y)}{\partial \epsilon_y} d\mathbf{c} = 0,$$

$$\int [\hat{\epsilon}_x(\mathbf{c}) - \epsilon_x] \frac{\partial \ln p(\mathbf{c}|\epsilon_x, \epsilon_y)}{\partial \epsilon_y} p(\mathbf{c}|\epsilon_x, \epsilon_y) d\mathbf{c} = 0. \tag{7}$$

Let  $Z, W, a_{11}, a_{12}, a_{21},$  and  $a_{22}$  be defined as follows:

$$Z \triangleq \left[ \frac{\hat{\epsilon}_x(\mathbf{c}) - \epsilon_x}{\frac{\partial \ln p(\mathbf{c}|\epsilon_x, \epsilon_y)}{\partial \epsilon_x}} \right], \tag{8}$$

$$W \triangleq \left[ \frac{\hat{\epsilon}_x(\mathbf{c}) - \epsilon_x}{\frac{\partial \ln p(\mathbf{c}|\epsilon_x, \epsilon_y)}{\partial \epsilon_x}} \right], \tag{9}$$

$$a_{11} \triangleq [\hat{\epsilon}_x(\mathbf{c}) - \epsilon_x], \tag{10}$$

$$a_{21} \triangleq \frac{\partial \ln p(\mathbf{c}|\epsilon_x, \epsilon_y)}{\partial \epsilon_x}, \tag{11}$$

$$a_{31} \triangleq \frac{\partial \ln p(\mathbf{c}|\epsilon_x, \epsilon_y)}{\partial \epsilon_y}. \tag{12}$$

From Eqs. (5) and (7) and expressions (11) and (12) one gets

$$\mathbf{E}[a_1 a_2] = 1, \tag{13}$$

$$\mathbf{E}[a_1 a_3] = 0, \tag{14}$$

where  $\mathbf{E}$  denotes the expectation operator. Furthermore, because a covariance matrix is always nonnegative definite it follows from expressions (8) and (9) and Eqs. (13) and (14) that

$$\det \mathbf{E}[ZZ^T] = \begin{vmatrix} \mathbf{E}[a_1^2] & 1 \\ 1 & \mathbf{E}[a_2^2] \end{vmatrix} \geq 0, \tag{15}$$

$$\det \mathbf{E}[WW^T] = \begin{vmatrix} \mathbf{E}[a_1^2] & 1 & 0 \\ 1 & \mathbf{E}[a_2^2] & \mathbf{E}[a_2 a_3] \\ 0 & \mathbf{E}[a_3 a_2] & \mathbf{E}[a_3^2] \end{vmatrix} > 0, \tag{16}$$

where  $\det$  denotes the matrix determinant operator.

It immediately follows from expressions (10) and (11) and Eq. (15) that

$$\mathbf{E}[a_1^2] \mathbf{E}[a_2^2] \geq 1,$$

$$\mathbf{E}[(\hat{\epsilon}_x(\mathbf{c}) - \epsilon_x)^2] \geq \frac{1}{\mathbf{E}\left[\left(\frac{\partial \ln p(\mathbf{c}|\epsilon_x, \epsilon_y)}{\partial \epsilon_x}\right)^2\right]}. \tag{17}$$

Equation (17) is the standard Cramér-Rao bound. Similarly from expressions (10)-(12) and Eq. (16) we have

$$\mathbf{E}[a_1^2] \begin{vmatrix} \mathbf{E}[a_2^2] & \mathbf{E}[a_2 a_3] \\ \mathbf{E}[a_3 a_2] & \mathbf{E}[a_3^2] \end{vmatrix} - \mathbf{E}[a_3^2] \geq 0$$

and

$$\mathbf{E}[(\hat{\epsilon}_x(\mathbf{c}) - \epsilon_x)^2] \geq \frac{\mathbf{E}\left\{\left[\frac{\partial \ln p(\mathbf{c}|\epsilon_x, \epsilon_y)}{\partial \epsilon_y}\right]^2\right\}}{\mathbf{E}\left\{\left[\frac{\partial \ln p(\mathbf{c}|\epsilon_x, \epsilon_y)}{\partial \epsilon_x}\right]^2\right\} \mathbf{E}\left\{\left[\frac{\partial \ln p(\mathbf{c}|\epsilon_x, \epsilon_y)}{\partial \epsilon_y}\right]^2\right\} - \left\{\mathbf{E}\left[\frac{\partial \ln p(\mathbf{c}|\epsilon_x, \epsilon_y)}{\partial \epsilon_x} \frac{\partial \ln p(\mathbf{c}|\epsilon_x, \epsilon_y)}{\partial \epsilon_y}\right]\right\}^2}. \tag{18}$$

Expression (18) is a 2-D version of the standard Cramér–Rao bound. Note that, in general, the Cramér–Rao bound is not the greatest lower bound.<sup>19</sup> It is, however, one of the few bounds that is mathematically tractable, and consequently it is used throughout the literature.

### IMAGE SPOT AT THE CHARGE-COUPLED DEVICE

The image spot at the CCD is assumed to have a Gaussian-shaped intensity profile  $S(x, y)$  and thus can be written as follows:

$$S(x, y, \epsilon_x, \epsilon_y) = (2\pi\sigma_s^2)^{-1} \exp\left[-\frac{(x - \epsilon_x)^2}{2\sigma_s^2}\right] \exp\left[-\frac{(y - \epsilon_y)^2}{2\sigma_s^2}\right], \quad (19)$$

where  $(\epsilon_x, \epsilon_y) \triangleq x$  and  $y$  coordinates of the center of the image spot at the CCD. For the 1-D case, Eq. (19) reduces to

$$S(x, \epsilon_x) = (2\pi\sigma_s^2)^{-1/2} \exp\left[-\frac{(x - \epsilon_x)^2}{2\sigma_s^2}\right], \quad (20)$$

$$S(y, \epsilon_y) = (2\pi\sigma_s^2)^{-1/2} \exp\left[-\frac{(y - \epsilon_y)^2}{2\sigma_s^2}\right]. \quad (21)$$

Note that

$$S(x, y, \epsilon_x, \epsilon_y) = S(x, \epsilon_x)S(y, \epsilon_y). \quad (22)$$

Let the center of the  $i$ - $j$ th pixel be given by  $x_i, y_j$ , and let this pixel be of size  $\Delta x$  by  $\Delta x$ . Then the average number of photoelectrons  $g_{ij}$  produced by this pixel because of the image spot is given by

$$g_{ij}(\epsilon_x, \epsilon_y) = \lambda_s g_i(\epsilon_x) g_j(\epsilon_y), \quad (23)$$

where

$$g_i(\epsilon_x) \triangleq \int_{x_i - \frac{\Delta x}{2}}^{x_i + \frac{\Delta x}{2}} S(x, \epsilon_x) dx, \quad (24)$$

$$g_j(\epsilon_y) \triangleq \int_{y_j - \frac{\Delta x}{2}}^{y_j + \frac{\Delta x}{2}} S(y, \epsilon_y) dy \quad (25)$$

$\lambda_s \triangleq$  average number of photoelectrons produced by the entire CCD array during the CCD integration time because of the image spot.

### ONE-DIMENSIONAL ESTIMATOR

The probability density of the output  $c_i$  of the  $i$ th pixel can be written in this case as

$$p(c_i|\epsilon_x) = \exp[-\lambda_s g_i(\epsilon_x) - \lambda_N] \frac{[\lambda_s g_i(\epsilon_x) + \lambda_N]^{c_i}}{c_i!}, \quad (26)$$

where  $\lambda_N \triangleq$  average number of dark-current photoelectrons produced by each CCD pixel during the CCD integration time.

It follows from Eq. (26) that

$$\begin{aligned} \ln p(\mathbf{c}|\epsilon_x) &= \ln \prod_i p(c_i|\epsilon_x) \\ &= - \sum_i [\lambda_s g_i(\epsilon_x) + \lambda_N] \\ &\quad - \sum_j \ln c_j! + \sum_i c_i \ln [\lambda_s g_i(\epsilon_x) + \lambda_N]. \end{aligned} \quad (27)$$

From Eq. (20) and expression (24) we have

$$\sum_i g_i(\epsilon_x) = 1, \quad (28)$$

and therefore

$$\Gamma \triangleq \frac{\partial \ln p(\mathbf{c}|\epsilon_x)}{\partial \epsilon_x} = \sum_i \frac{c_i \lambda_s g_i'(\epsilon_x)}{\lambda_s g_i(\epsilon_x) + \lambda_N}, \quad (29)$$

where

$$g_i'(\epsilon_x) \triangleq \frac{\partial}{\partial \epsilon_x} g_i(\epsilon_x).$$

From Eq. (29) it follows that

$$\begin{aligned} \mathbf{E}[\Gamma^2] &= \sum_i \left[ \frac{\lambda_s g_i'(\epsilon_x)}{\lambda_s g_i(\epsilon_x) + \lambda_N} \right]^2 \mathbf{E}[c_i^2] \\ &\quad + \sum_{i \neq j} \frac{\lambda_s g_i'(\epsilon_x)}{\lambda_s g_i(\epsilon_x) + \lambda_N} \frac{\lambda_s g_j'(\epsilon_x)}{\lambda_s g_j(\epsilon_x) + \lambda_N} \mathbf{E}[c_i] \mathbf{E}[c_j]. \end{aligned} \quad (30)$$

Because  $c_i$  is Poisson distributed with mean  $\lambda_s g_i(\epsilon_x) + \lambda_N$  we have

$$\mathbf{E}[c_i] = \lambda_s g_i(\epsilon_x) + \lambda_N, \quad (31)$$

$$\mathbf{E}[c_i^2] = [\lambda_s g_i(\epsilon_x) + \lambda_N][1 + \lambda_s g_i(\epsilon_x) + \lambda_N]. \quad (32)$$

Combining expression (29) and Eqs. (30) and (31) yields

$$\mathbf{E}[\Gamma^2] = \left[ \sum_i \lambda_s g_i'(\epsilon_x) \right]^2 + \sum_i \frac{[\lambda_s g_i'(\epsilon_x)]^2}{\lambda_s g_i(\epsilon_x) + \lambda_N}. \quad (33)$$

From Eq. (20) and expression (24) it is easy to show that

$$\sum_i g_i'(\epsilon_x) = 0, \quad (34)$$

and therefore by expressions (17) and (29) and Eqs. (33) and (34) it follows that

$$\begin{aligned} \mathbf{E}[(\hat{\epsilon}_x(\mathbf{c}) - \epsilon_x)^2] &\geq \frac{1}{\mathbf{E}[\Gamma^2]} \\ &= \frac{1}{\sum_i \frac{[\lambda_s g_i'(\epsilon_x)]^2}{\lambda_s g_i(\epsilon_x) + \lambda_N}}. \end{aligned} \quad (35)$$

Expression (35) represents the Cramér–Rao lower bound for an unbiased estimator of  $\epsilon_x$ . Also note that the maximum-likelihood estimate of position is that value of  $\epsilon_x$  for

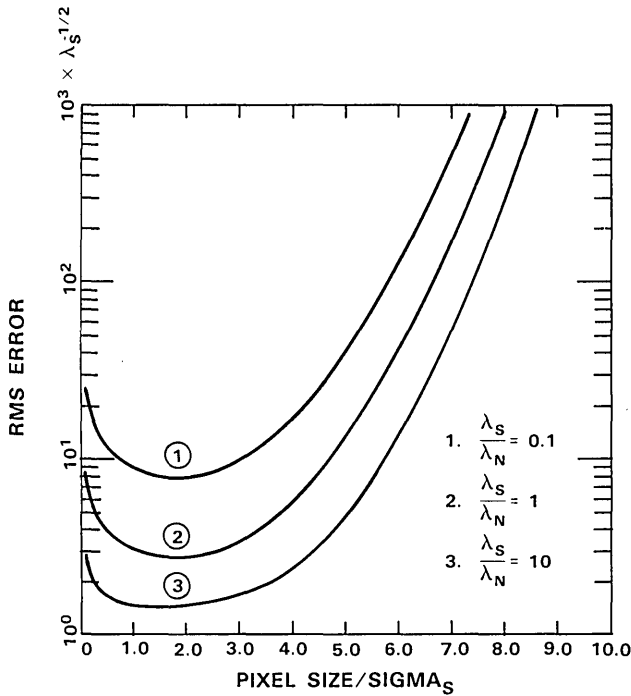


Fig. 1. Lower bound on performance of 1-D CCD optical position estimator.

which  $\Gamma = 0$  [see expression (29)], and at large signal-to-noise ratios (i.e.,  $\lambda_s/\lambda_N \gg 1$ ) this estimator is independent of  $\lambda_s$  and  $\lambda_N$ . Because the center of the image spot (i.e.,  $\epsilon_x$ ) is unknown and equally likely to lie anywhere on the array, expression (35) can be averaged over the entire array region, thus yielding a lower bound on the average mean-squared error. It is necessary, however, to perform the averaging over only the following one-pixel region:

$$\frac{-\Delta x}{2} \leq \epsilon_x \leq \frac{\Delta x}{2}$$

because the array has a periodic structure. This fact can be understood by noting that for a CCD of infinite extent an observer cannot distinguish the physical difference when the center of the spot is translated by an integer number of pixels. Therefore

$$\frac{1}{\sum_i \frac{[\lambda_s g'_i(\epsilon_x)]^2}{\lambda_s g_i(\epsilon_x) + \lambda_N}} = \frac{1}{\sum_i \frac{[\lambda_s g'_i(\epsilon_x + n\Delta x)]^2}{\lambda_s g_i(\epsilon_x + n\Delta x) + \lambda_N}}$$

for all integers  $n$ .

Thus, averaging the left-hand side of the above equation over  $-\infty$  to  $+\infty$  is equivalent to averaging it over  $-\Delta x/2$  to  $+\Delta x/2$ . That is,

$$\lim_{L \rightarrow \infty} \frac{1}{L} \int_{-L/2}^{L/2} \frac{1}{\sum_i \frac{[\lambda_s g'_i(\epsilon_x)]^2}{\lambda_s g_i(\epsilon_x) + \lambda_N}} d\epsilon_x = \frac{1}{\Delta x} \int_{-\Delta x/2}^{\Delta x/2} \frac{1}{\sum_i \frac{[\lambda_s g'_i(\epsilon_x)]^2}{\lambda_s g_i(\epsilon_x) + \lambda_N}} d\epsilon_x.$$

Of course if the CCD array is of finite extent then the equali-

ty above is not strictly true but is nearly so, provided that (1) the spot size is small compared with the total size of the CCD and (2) the spot does not lie at the edge of the array. Note that if condition (1) is met (and it usually is in practice), then condition (2) will also be met with high probability.

The normalized rms position error is defined below:

normalized rms error<sub>1-D</sub>

$$= \left[ \frac{1}{\Delta x} \int_{-\Delta x/2}^{\Delta x/2} \frac{E[(\hat{\epsilon}_x(\mathbf{c}) - \epsilon_x)^2] d\epsilon_x}{\sigma_s} \right]^{1/2}. \quad (36)$$

By using expression (35) and Eq. (36), Fig. 1 plots a lower bound for the normalized rms error (1-D case) versus the pixel-to-image size ratio  $\Delta x/\sigma_s$ . We note from Fig. 1 that the pixel-to-image size ratio at which the lower bound is minimum lies between 1 and 2 for a wide range of signal-to-noise ratios. Furthermore, the lower bound does not vary significantly for ratios between 1 and 2. Finally, we note that the rms error is a function of both the signal power and noise power separately and not just their ratio  $\lambda_s/\lambda_N$ . This type of behavior is characteristic of systems whose performance is governed by Poisson statistics.

### TWO-DIMENSIONAL ESTIMATOR

The probability density of the output  $c_{ij}$  of the  $i$ - $j$ th pixel can be written in this case as

$$p(c_{ij} | \epsilon_x, \epsilon_y) = \exp[-\lambda_s g_i(\epsilon_x) g_j(\epsilon_y) - \lambda_N] \frac{[\lambda_s g_i(\epsilon_x) g_j(\epsilon_y) + \lambda_N]^{c_{ij}}}{c_{ij}!}. \quad (37)$$

It follows from Eq. (37) that

$$\begin{aligned} \ln p(\mathbf{c} | \epsilon_x, \epsilon_y) &= \ln \prod_{ij} p(c_{ij} | \epsilon_x, \epsilon_y) \\ &= - \sum_{ij} [\lambda_s g_i(\epsilon_x) g_j(\epsilon_y) + \lambda_N] - \sum_{ij} \ln c_{ij}! \\ &\quad + \sum_{ij} c_{ij} \ln [\lambda_s g_i(\epsilon_x) g_j(\epsilon_y) + \lambda_N]. \end{aligned} \quad (38)$$

From Eqs. (19)–(23) and expressions (24) and (25) we have

$$\sum_{ij} g_i(\epsilon_x) g_j(\epsilon_y) = 1, \quad (39)$$

and therefore

$$Q_x \triangleq \frac{\partial \ln p(\mathbf{c} | \epsilon_x, \epsilon_y)}{\partial \epsilon_x} = \sum_{ij} c_{ij} \frac{\lambda_s g'_i(\epsilon_x) g_j(\epsilon_y)}{\lambda_s g_i(\epsilon_x) g_j(\epsilon_y) + \lambda_N}, \quad (40)$$

$$Q_y \triangleq \frac{\partial \ln p(\mathbf{c} | \epsilon_x, \epsilon_y)}{\partial \epsilon_y} = \sum_{ij} c_{ij} \frac{\lambda_s g_i(\epsilon_x) g'_j(\epsilon_y)}{\lambda_s g_i(\epsilon_x) g_j(\epsilon_y) + \lambda_N}, \quad (41)$$

where

$$g'_i(\epsilon_x) \triangleq \frac{\partial}{\partial \epsilon_x} g_i(\epsilon_x)$$

and

$$g'_j(\epsilon_y) \triangleq \frac{\partial}{\partial \epsilon_y} g_j(\epsilon_y).$$

From Eqs. (40) and (41) it follows that

$$\begin{aligned} \mathbf{E}[Q_x^2] &= \sum_{ij} \left[ \frac{\lambda_s g'_i(\epsilon_x) g_j(\epsilon_y)}{\lambda_s g_i(\epsilon_x) g_j(\epsilon_y) + \lambda_N} \right]^2 \mathbf{E}[c_{ij}^2] \\ &+ \sum_{ij} \sum_{nm \neq ij} \frac{\lambda_s g'_i(\epsilon_x) g_j(\epsilon_y)}{\lambda_s g_i(\epsilon_x) g_j(\epsilon_y) + \lambda_N} \\ &\times \frac{\lambda_s g'_n(\epsilon_x) g_m(\epsilon_y)}{\lambda_s g_n(\epsilon_x) g_m(\epsilon_y) + \lambda_N} \mathbf{E}[c_{ij}] \mathbf{E}[c_{nm}], \end{aligned} \quad (42)$$

$$\begin{aligned} \mathbf{E}[Q_x Q_y] &= \sum_{ij} \frac{\lambda_s g'_i(\epsilon_x) g_j(\epsilon_y)}{\lambda_s g_i(\epsilon_x) g_j(\epsilon_y) + \lambda_N} \frac{\lambda_s g'_i(\epsilon_x) g'_j(\epsilon_y)}{\lambda_s g_i(\epsilon_x) g_j(\epsilon_y) + \lambda_N} \mathbf{E}[c_{ij}^2] \\ &+ \sum_{ij} \sum_{nm \neq ij} \frac{\lambda_s g'_i(\epsilon_x) g_j(\epsilon_y)}{\lambda_s g_i(\epsilon_x) g_j(\epsilon_y) + \lambda_N} \\ &\times \frac{\lambda_s g'_n(\epsilon_x) g'_m(\epsilon_y)}{\lambda_s g_n(\epsilon_x) g'_m(\epsilon_y) + \lambda_N} \mathbf{E}[c_{ij}] \mathbf{E}[c_{nm}], \end{aligned} \quad (43)$$

Combining Eqs. (42)–(46) yields

$$\mathbf{E}[Q_x^2] = \left[ \sum_{ij} \lambda_s g'_i(\epsilon_x) g_j(\epsilon_y) \right]^2 + \sum_{ij} \frac{[\lambda_s g'_i(\epsilon_x) g_j(\epsilon_y)]^2}{\lambda_s g_i(\epsilon_x) g_j(\epsilon_y) + \lambda_N}, \quad (47)$$

$$\begin{aligned} \mathbf{E}[Q_x Q_y] &= \sum_{ij} \lambda_s g'_i(\epsilon_x) g_j(\epsilon_y) \sum_{nm} \lambda_s g'_n(\epsilon_x) g'_m(\epsilon_y) \\ &+ \sum_{ij} \frac{\lambda_s^2 g'_i(\epsilon_x) g'_j(\epsilon_y) g_i(\epsilon_x) g_j(\epsilon_y)}{\lambda_s g_i(\epsilon_x) g_j(\epsilon_y) + \lambda_N}, \end{aligned} \quad (48)$$

$$\mathbf{E}[Q_y^2] = \left[ \sum_{ij} \lambda_s g_i(\epsilon_x) g'_j(\epsilon_y) \right]^2 + \sum_{ij} \frac{[\lambda_s g_i(\epsilon_x) g'_j(\epsilon_y)]^2}{\lambda_s g_i(\epsilon_x) g_j(\epsilon_y) + \lambda_N}. \quad (49)$$

From Eqs. (20) and (21) and expressions (24) and (25) it is easy to show that

$$\sum_{ij} g'_i(\epsilon_x) g_j(\epsilon_y) = \sum_{ij} g_i(\epsilon_x) g'_j(\epsilon_y) = 0, \quad (50)$$

and therefore by expressions (18), (40), and (41) and Eqs. (47)–(50) it follows that

$$\begin{aligned} \mathbf{E}[(\hat{\epsilon}_x(c) - \epsilon_x)^2] &\geq \frac{\mathbf{E}[Q_y^2]}{\mathbf{E}[Q_x^2] \mathbf{E}[Q_y^2] - (\mathbf{E}[Q_x Q_y])^2} \\ &= \frac{\left\{ \sum_{ij} \frac{[\lambda_s g'_i(\epsilon_x) g'_j(\epsilon_y)]^2}{\lambda_s g_i(\epsilon_x) g_j(\epsilon_y) + \lambda_N} \right\}}{\left\{ \sum_{ij} \frac{[\lambda_s g'_i(\epsilon_x) g_j(\epsilon_y)]^2}{\lambda_s g_i(\epsilon_x) g_j(\epsilon_y) + \lambda_N} \sum_{ij} \frac{[\lambda_s g_i(\epsilon_x) g'_j(\epsilon_y)]^2}{\lambda_s g_i(\epsilon_x) g_j(\epsilon_y) + \lambda_N} - \left[ \sum_{ij} \frac{\lambda_s^2 g'_i(\epsilon_x) g'_j(\epsilon_y) g_i(\epsilon_x) g_j(\epsilon_y)}{\lambda_s g_i(\epsilon_x) g_j(\epsilon_y) + \lambda_N} \right]^2 \right\}} \\ &= \frac{\lambda_s^{-1}}{\sum_{ij} \frac{[g'_i(\epsilon_x) g_j(\epsilon_y)]^2}{g_i(\epsilon_x) g_j(\epsilon_y) + (\lambda_s/\lambda_N)^{-1}} - \frac{\left[ \sum_{ij} \frac{g'_i(\epsilon_x) g_j(\epsilon_y) g_i(\epsilon_x) g'_j(\epsilon_y)}{g_i(\epsilon_x) g_j(\epsilon_y) + (\lambda_s/\lambda_N)^{-1}} \right]^2}{\sum_{ij} \frac{g_i(\epsilon_x) g'_j(\epsilon_y)}{g_i(\epsilon_x) g_j(\epsilon_y) + (\lambda_s/\lambda_N)^{-1}}}}. \end{aligned} \quad (51)$$

$$\begin{aligned} \mathbf{E}[Q_y^2] &= \sum_{ij} \left[ \frac{\lambda_s g_i(\epsilon_x) g'_j(\epsilon_y)}{\lambda_s g_i(\epsilon_x) g_j(\epsilon_y) + \lambda_N} \right]^2 \mathbf{E}[c_{ij}^2] \\ &+ \sum_{ij} \sum_{nm \neq ij} \frac{\lambda_s g_i(\epsilon_x) g'_j(\epsilon_y)}{\lambda_s g_i(\epsilon_x) g_j(\epsilon_y) + \lambda_N} \\ &\times \frac{\lambda_s g_n(\epsilon_x) g'_m(\epsilon_y)}{\lambda_s g_n(\epsilon_x) g'_m(\epsilon_y) + \lambda_N} \mathbf{E}[c_{ij}] \mathbf{E}[c_{nm}]. \end{aligned} \quad (44)$$

Since  $c_{ij}$  is Poisson distributed with mean  $\lambda_s g_i(\epsilon_x) g_j(\epsilon_y) + \lambda_N$  we have

$$\mathbf{E}[c_{ij}] = \lambda_s g_i(\epsilon_x) g_j(\epsilon_y) + \lambda_N, \quad (45)$$

$$\mathbf{E}[c_{ij}^2] = [\lambda_s g_i(\epsilon_x) g_j(\epsilon_y) + \lambda_N][1 + \lambda_s g_i(\epsilon_x) g_j(\epsilon_y) + \lambda_N]. \quad (46)$$

Expression (51) represents a 2-D Cramér–Rao lower bound for an unbiased estimate of  $\epsilon_x$ . Also note that the values of  $\epsilon_x$  and  $\epsilon_y$  for which  $Q_x$  and  $Q_y$  are zero [see expressions (40) and (41)] are the maximum-likelihood estimates of position, and at large signal-to-noise ratios (i.e.,  $\lambda_s/\lambda_N \gg 1$ ) these estimates are independent of  $\lambda_s$  and  $\lambda_N$ . Because the center of the image spot (i.e.,  $\epsilon_x$ ,  $\epsilon_y$ ) is unknown and equally likely to lie anywhere on the CCD, expression (51) will now be averaged over the uncertainty region, thus yielding a lower bound on the average mean-squared error. As in the 1-D case, the averaging will be performed over a one-pixel region:

$$-\frac{\Delta x}{2} \leq \epsilon_x \leq \frac{\Delta x}{2}, \quad -\frac{\Delta y}{2} \leq \epsilon_y \leq \frac{\Delta y}{2}.$$

The normalized rms position error obtained from this average is defined below:

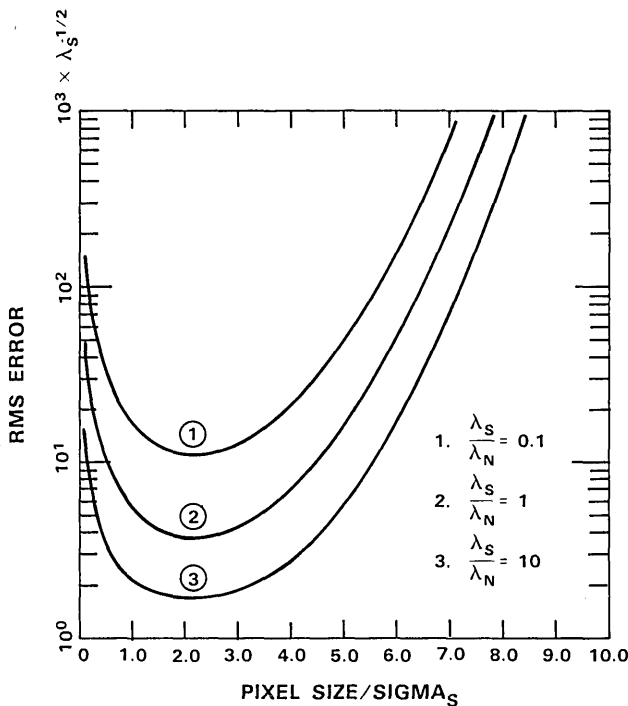


Fig. 2. Lower bound on performance of 2-D CCD optical position estimator.

normalized rms error<sub>2-D</sub>

$$= \frac{\left[ \frac{1}{(\Delta x)^2} \int_{-\Delta x/2}^{\Delta x/2} \int_{-\Delta x/2}^{\Delta x/2} \mathbf{E}[\hat{\epsilon}_x(\mathbf{c}) - \epsilon_x]^2 d\epsilon_x d\epsilon_y \right]^{1/2}}{\sigma_s} \quad (52)$$

By using expression (51) and Eq. (52), Fig. 2 plots a lower bound for the normalized rms error (2-D case) versus the pixel-to-image size ratio  $\Delta x/\sigma_s$ . We note from Fig. 2 that the pixel-to-image size ratio at which the lower bound is minimum lies between 1.5 and 2.5 for a wide range of signal-to-noise ratios. Furthermore, the lower bound does not vary significantly between 1.5 and 2.5. Finally, note that although the normalized rms error in the  $x$  direction was derived above, an identical result is easily obtained for the  $y$  direction.

## CONCLUSIONS

The problem of optically estimating an object's position by using a CCD array composed of square pixels  $\Delta x$  on a side has been analyzed. The object's image spot at the CCD was assumed to have a Gaussian intensity profile with the  $1/e$  point at a radial distance of  $\sqrt{2}\sigma_s$  from the peak, and the CCD noise was modeled as Poisson-distributed dark-current shot noise. A 2-D Cramér-Rao bound was developed and used to determine a lower limit for the mean-squared error of any unbiased position estimator, and the maximum-likelihood estimator was also derived. For the 1-D position-estimation problem the lower bound was minimum, over a wide range of signal-to-noise ratios, for a pixel-to-image spot size ratio (i.e.,  $\Delta x/\sigma_s$ ) of between 1 and 2. Similarly for the 2-D problem, the lower bound was minimum for a pixel-to-image spot size ratio of between 1.5 and 2.5. In both cases the lower bound was relatively insensitive to  $\Delta x/\sigma_s$  in the region of its

minimum. It was also observed that the lower bound is a function of both the signal power and noise power separately and not just of their ratio. It was noted that this type of behavior is characteristic of systems whose performance is governed by Poisson statistics. Finally, at high signal-to-noise ratios the maximum-likelihood estimator was shown to be independent of the signal and noise powers.

## ACKNOWLEDGMENT

This work was sponsored by the U.S. Department of the Air Force.

## REFERENCES

1. R. Stanton, J. Alexander, E. Dennison, T. Glavich, P. Salomon, and R. Williamson, "ASTROS: a sub-arcsec CCD star tracker," in *State of the Art Imaging Arrays and their Applications*, K. N. Prettyjohns, ed., Proc. Soc. Photo-Opt. Instrum. Eng. **501**, 256-282 (1984).
2. P. Salomon and T. Glavich, "Image signal processing in subpixel accuracy star trackers," in *Smart Sensors. II*, B. S. Barbe, ed., Proc. Soc. Photo-Opt. Instrum. Eng. **252**, 64-74 (1980).
3. J. Cox, "Evaluation of peak location algorithms with subpixel accuracy for mosaic focal planes," in *Processing of Images and Data from Optical Sensors*, W. H. Carter, ed., Proc. Soc. Photo-Opt. Instrum. Eng. **292**, 288-299 (1981).
4. E. Dennison and R. Stanton, "Ultra-precise star tracking using charged coupled devices (CCDs)," in *Smart Sensors. II*, B. S. Barbe, ed., Proc. Soc. Photo-Opt. Instrum. Eng. **252**, 54-63 (1980).
5. P. Salomon and W. Goss, "A microprocessor-controlled CCD star tracker," presented at the AIAA 14th Aerospace Sciences Meeting, Washington, D.C., 1976.
6. J. Kollodge and J. Sand, "Advanced star tracker design using the charge injection device," presented at the Annual Rocky Mountain Guidance and Control Convention, Keystone, Colo., 1982.
7. S. Grossman and R. Emmons, "Performance analysis and size optimization of focal planes for point-source tracking algorithm applications," Opt. Eng. **23**, 167-176 (1984).
8. D. Snyder and P. Fishman, "How to track a swarm of fireflies by observing their flashes," IEEE Trans. Inf. Theory **IT-10**, 692-695 (1975).
9. C. Helstrom, "The detection and resolution of optical signals," IEEE Trans. Inf. Theory **IT-10**, 275-287 (1964).
10. E. Farrell and C. Zimmerman, "Information limits of scanning optical systems," in *Optical and Electro-Optical Information Processing*, J. T. Tippet, D. A. Berkowitz, L. C. Clapp, C. J. Koester, and A. Vanderburgh, Jr., eds. (MIT Press, Cambridge, Mass., 1965), Chap. 35.
11. T. McGarty, "The estimation of the center of gravity of a photon density profile in noise," IEEE Trans. Aerosp. Electron. Syst. **AES-5**, 974-979 (1969).
12. M. Elbaum and P. Diamant, "Estimation of image centroid, size and orientation with laser radar," Appl. Opt. **16**, 2433-2437 (1977).
13. M. Elbaum and M. Greenebaum, "Annular apertures for angular tracking," Appl. Opt. **16**, 2438-2440 (1977).
14. M. Elbaum, P. Diamant, M. King, and W. Edelson, "Maximum angular accuracy of pulsed laser radar in photocounting limit," Appl. Opt. **16**, 1982-1992 (1977).
15. D. Lubnau, "Maximum likelihood estimate of target angles for a conical scan tracking system in the presence of speckle," Appl. Opt. **16**, 184-186 (1977).
16. L. Kazovsky, "Beam position estimation by means of detector arrays," Opt. Quantum Electron. **13**, 201-208 (1981).
17. D. L. Snyder, *Random Point Process* (Wiley, New York, 1975).
18. L. D. Vilesov and V. N. Veis, "Estimate of the angular position

- of a source of light when received by an array of photodetectors," *Izv. Vyssh. Uchebn. Zaved. Radioelektron.* **26**, 85-87 (1983).
19. H. Van Trees, *Detection, Estimation and Modulation Theory* (Wiley, New York, 1968), Part I.
  20. C. W. Chen, "Optical Tracking Systems," Ph.D. dissertation (Washington University, St. Louis, Missouri, 1982).
  21. C. W. Chen and D. L. Snyder, "A lower bound on the estimation performance for stochastic control systems," *IEEE Trans. Autom. Control* **AC-29**, 577-559 (1984).